Journal of Machine Learning Research 21 (2020) 1-26 Submitted 6/13; Published 7/20

# Bayesian Closed Surface Fitting Through Tensor Products

**Olivier Binette** OLIVIER.BINETTE@DUKE.EDU
*Department of Statistical Science*
*Duke University*
*Durham, NC 27708-0251, USA*

**Debdeep Pati** DEBDEEP@STAT.TAMU.EDU
*Department of Statistics*
*Texas A&M University*
*College Station, TX 77843, USA*

**David B. Dunson** DUNSON@STAT.DUKE.EDU
*Department of Statistical Science*
*Duke University*
*Durham, NC 27708-0251, USA*

**Editor:** François Caron

## Abstract

Closed surfaces provide a useful model for 3-d shapes, with the data typically consisting of a cloud of points in $\mathbb{R}^3$. The existing literature on closed surface modeling focuses on frequentist point estimation methods that join surface patches along the edges, with surface patches created via Bézier surfaces or tensor products of B-splines. However, the resulting surfaces are not smooth along the edges and the geometric constraints required to join the surface patches lead to computational drawbacks. In this article, we develop a Bayesian model for closed surfaces based on tensor products of a cyclic basis resulting in infinitely smooth surface realizations. We impose sparsity on the control points through a double-shrinkage prior. Theoretical properties of the support of our proposed prior are studied and it is shown that the posterior achieves the optimal rate of convergence under reasonable assumptions on the prior. The proposed approach is illustrated with some examples.

**Keywords:** 3-d shapes; Bayesian nonparametrics; Imaging; Manifold learning; Splines; Tensors.

## 1. Introduction

Surface reconstruction can be viewed as an algorithm that takes as an input an unorganized set of points $\{p_1, \ldots, p_n\} \in \mathbb{R}^3$ on or near an unknown manifold $\mathcal{M}$ embedded in $\mathbb{R}^3$ and produces a surface that approximates $\mathcal{M}$. Free-form surface modeling from massive data points is becoming an important area of research in commercial computer aided design and development of manufacturing software (Barnhill, 1985; Lang and Röschel, 1992; Hagen and Santarelli, 1992; Aziz et al., 2002). A collection of introductory works on surface modeling can be found in Su and Liu (1989) and the subsequent developments in Muller (2005).

Common surface reconstruction algorithms in the computer science literature usually follow a sequential multistage process which includes scanning, outlier removal, denoising and input normal estimation to generate a simplicial surface. The Poisson surface reconstruction method (Kazhdan et al., 2006) solves for an approximate indicator function of the inferred surface, whose gradient best matches the input normals. The output scalar function, represented in an adaptive octree (Whang et al., 2002), is then iso-contoured using an adaptive marching cubes algorithm (Lorensen and Cline, 1987). CGAL surface mesh generator (Rineau and Yvinec, 2007) implements a variant of this algorithm which solves for a piecewise linear function on a 3D Delaunay triangulation instead of an adaptive octree. Hoppe et al. (1992); Boissonnat and Oudot (2005) developed a two stage surface reconstruction algorithm by first estimating $\mathcal{M}$ by the implicit surface $Z(f) = \{y : f(y) = 0\}$ of a suitable function $f : \mathbb{R}^3 \to \mathbb{R}$ and then using a contouring algorithm to approximate $Z(f)$ by a simplicial surface.

There is a rich literature on estimation of surfaces using tensor products of bases (Fowler, 1992; Goshtasby, 1992; Mann and DeRose, 1995; Johnstone and Sloan, 1995). Tensor product surfaces provide a flexible representation of a surface embedded in an arbitrary Euclidean space. However, there is a limited literature on Bayesian modeling of free-form surfaces (Cunningham et al., 1999) and closed surfaces (Soussen and Mohammad-Djafari, 2002). While frequentist surface estimation using tensor products has been widely studied, Bayesian estimation has received almost no consideration. A notable exception is the approach of Smith and Kohn (1997) for Bayesian estimation of bivariate regression surfaces using tensor products. However estimating a parametric surface $S(u, v) : \mathcal{D}_2 \to \mathbb{R}^3$, where $\mathcal{D}_2 \subset \mathbb{R}^2$ is different from usual regression surface or function estimation because the independent variable $(u, v)$ is unknown.

Modeling of closed surfaces is a primary focus in application areas such as computer vision, as closed surfaces provide an adequate geometric model of a wide range of objects ranging from anatomical organs to machine parts. In this field, standard practice involves restrictive parametric shapes depending on a few parameters (Cinquin et al., 1982; Amenta et al., 1998; Rossi and Willsky, 2003). Although such models can describe many common surfaces, the variety of generated shapes is limited. More flexible models for closed surfaces can be defined through carefully specified linear combinations of basis functions. Soussen and Mohammad-Djafari (2002) developed the notion of global harmonic surfaces, which yield a simple procedure to reconstruct coarse surfaces. Shen and Makedon (2006); Chung et al. (2008) developed a novel method based on general and weighted spherical harmonics to model closed sphere-like objects, such as the cortical surface. However the variety of shapes generated by spherical harmonics are somewhat limited to sphere-like or convex objects although weighted spherical harmonics can capture local features like cortical folds quite well.

Amenta et al. (1998) developed a surface reconstruction algorithm called the Crust algorithm based on the three-dimensional Voronoi diagram to model closed surfaces from a data cloud in $\mathbb{R}^3$. The algorithm generates a regular surface and the output mesh interpolates, rather than approximates, the input points. However, the algorithm is not probabilistic and does not allow uncertainty in estimating the surface. Moreover, the algorithm requires a dense collection of data points for a reasonably good reconstruction indicating slow convergence. Some illustrations of the Crust algorithm are provided in Fig. 1. In computer aided design, closed surface modeling is often aided by combining several Bézier or spline surface patches by endpoint interpolation (Gordon and Riesenfeld, 1974; Piegl, 1986; Casale, 1987; Szeliski and Tonnesen, 1992; Hoppe et al., 1992; Yang and Lee, 1999; Li et al., 2007). In

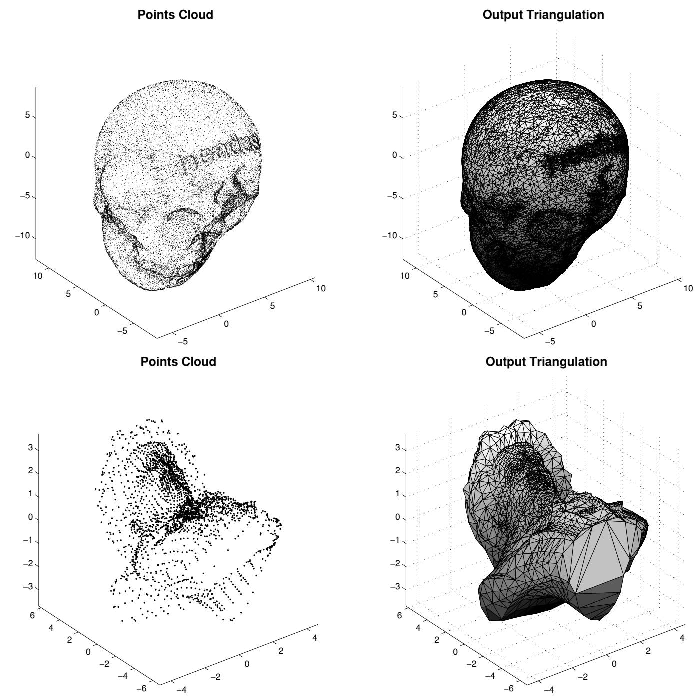


Figure 1: Output triangulation from crust algorithm on a point cloud

a frequentist analysis such endpoint restrictions are incorporated through constrained optimization. In the Bayesian paradigm, these restrictions lead to mixing problems in the posterior analysis. Furthermore, these restrictions can make the resulting surface non-differentiable along the edges joining the patches.

We instead use a cyclic basis developed by Róth et al. (2009) to accommodate restrictions without parameter constraints and give rise to an infinitely smooth surface. We propose a Bayesian hierarchical model of a closed surface embedded in $\mathbb{R}^3$ using tensor products of such cyclic bases with a carefully-chosen shrinkage prior placed on the tensor of basis coefficients. In particular, motivated by the decreasing impact of the higher indexed basis functions in the Bézier surface representation, we increasingly shrink the higher indexed coefficients. The specification leads to a highly efficient algorithm for posterior computation that allows uncertainty in the number of bases. In addition, the proposed prior is shown to have large support and to lead to a posterior with the optimal rate of convergence up to a log factor.

## 2. Outline of the Method

### 2.1. Review of Terminology

Assume a data cloud $\{p_i \in \mathbb{R}^3, i = 1, \ldots, N\}$ is given. Our aim is to obtain a posterior distribution for a smooth closed surface about which these data points are concentrated. Before going into the details of our model, we start with a few definitions.

**Definition 1** *A closed surface is a compact two dimensional closed manifold which does not have a boundary. Examples are spaces like the sphere, torus, Klein bottle etc.*

**Definition 2** *A parametric surface is a surface in $\mathbb{R}^3$ which is defined by a parametric equation with two parameters $u$ and $v$. Mathematically, a parametric surface is an injective map from $\mathbb{R}^2$ to $\mathbb{R}^3$ defined by $S : [a, b]^2 \to \mathbb{R}^3, (u, v) \mapsto S(u, v)$. See the Purdue University thesis Sederberg (1983) for a detailed description of parametric surfaces.*

**Definition 3** *A tensor product surface is formed by taking a tensor product of bases*

$$S_{n,m}(u, v) = \sum_{j=0}^{k_n} \sum_{k=0}^{k_m} d_{jk} B_j^n(u) B_k^m(v), \tag{1}$$

*where $(u, v) \in [a, b]^2$, $\{d_{jk} \in \mathbb{R}^3, j = 0, \ldots, k_m, k = 0, \ldots, k_n\}$ are control points and $\{B_l^{k_n}(u), u \in [a, b], l = 0, \ldots, k_n\}$ are basis functions.*

Here $k_n = n$ or $2n$ depending on whether the bases span the algebraic or the trigonometric polynomials having maximum degree $n$. An example of a tensor product surface is the *Bézier* surface (Farin, 2002) in which $B_j^n(u) = \binom{n}{j} u^j (1 - u)^{n-j}, j = 1, \ldots, n, u \in [0, 1]$. Bézier surfaces are an extension of the idea of Bézier curves, and share many of their properties.

### 2.2. Closed Surface Model

We assume that the data $\{p_i = (p_i^1, p_i^2, p_i^3)^{\mathrm{T}}, i = 1, \ldots, N\}$ arise as a random additive perturbation from a closed parametric surface $S(u, v)$, $(u, v) \in [-\pi, \pi]^2$, as follows,

$$p_i = S(u_i, v_i) + e_i, \quad e_i \sim \mathrm{N}(0, \sigma^2 I_3), \quad i = 1, \ldots, N, \tag{2}$$

$$(u_i, v_i) \sim \Pi_{[-\pi,\pi]^2} \tag{3}$$

where $(u_i, v_i)$ are coordinates in $[-\pi, \pi]^2$ corresponding to $p_i \in \mathbb{R}^3$, $S(u_i, v_i) = \{S^1(u_i, v_i), S^2(u_i, v_i), S^3(u_i, v_i)\}^{\mathrm{T}}$ is the unknown surface at coordinates $(u_i, v_i)$, $e_i \in \mathbb{R}^3$ is a measurement error and $\Pi_{[-\pi,\pi]^2}$ is a probability distribution on $[-\pi, \pi]^2$. In absence of any information on the coordinates, one can let $(u_i, v_i) \sim \mathrm{Unif}([-\pi, \pi]^2)$. Let $P$ denote the $N \times 3$ matrix representation with rows $\{p_i^{\mathrm{T}}, i = 1, \ldots, N\}$. Assume $\sigma^{-2} \sim \mathrm{Ga}(a_\sigma, b_\sigma)$. We follow a *tensor product surface* representation (1) to model the closed parametric surface $S(u, v), (u, v) \in [-\pi, \pi]^2$.

In §3, the coordinates $(u_i, v_i)$, $i = 1, \ldots, N$, are assumed to be known. They are obtained through a parameterization step described in §4.

### 2.3. Construction of a Closed Surface Using a Cyclic Basis

Using the tensor product specification in (1) for the surface $S(u, v)$, we propose to use the cyclic basis developed by Róth et al. (2009); Róth and Juhász (2010). These bases have a cyclic symmetry that eliminates the need for constraints on the control points, while also leading to surfaces that are infinitely smooth in the sense that the realizations are infinitely differentiable ($C^\infty$). Assuming $S \in C^\infty$ is appealing in avoiding the need for geometric constraints and surfaces in $C^\infty$ can approximate any parametric closed surface arbitrarily well preserving local features. In addition, $S$ can be characterized as a single coherent surface depending only on the control points, unlike piecing together local surfaces with heavy geometric constraints along the joints.

Róth et al. (2009) devised a basis for the vector space

$$\mathcal{V}_n = \langle 1, \cos(u), \sin(u), \ldots, \cos(nu), \sin(nu) \rangle$$

of trigonometric polynomials of degree at most $n$, i.e., of truncated Fourier series. Let

$$B_j^n(u) = \frac{c_n}{2^n} \left\{ 1 + \cos\left( u + \frac{2\pi j}{2n+1} \right) \right\}^n, \quad (j = 0, 1, \ldots, 2n), u \in [-\pi, \pi], \tag{4}$$

where $c_n = \frac{(2^n n!)^2}{(2n+1)!}$. The following lemma from Róth et al. (2009) demonstrates that any truncated Fourier series can be expressed as a linear combination of the $B_j^n$ for some large $n$. This implies that any reasonable closed curve can be approximated arbitrarily well by the linear combination of the $B_j^n$ for some $n$. This concept is formalized in §3 in discussing posterior convergence.

**Lemma 4** *The functions $\{B_j^n(u), j = 0, 1, \ldots, 2n, u \in [-\pi, \pi]\}$ form a basis of the vector space $\mathcal{V}_n$.*

Using basis functions (4), we can define the tensor product of surfaces of degree $(n, m)(n \geq 1, m \geq 1)$ by $S_{n,m}(u, v)$ with $k_n = 2n$ in (1). Lemma 5 guarantees that $S_{n,m}$ is closed for any choice of $\{d_{jk}, j = 0, \ldots, 2n, k = 0, \ldots, 2m\}$ in (1).

**Lemma 5** *The tensor product surface $S_{n,m} : [-\pi, \pi]^2 \to \mathbb{R}^3$ constructed using basis functions (4) is closed.*

**Proof** If not, there exists a boundary of the surface, i.e., there exists a neighborhood $U_T$ of the torus $[-\pi, \pi]^2$ which is not entirely mapped to the surface $S_{n,m}$. Since the inside of $[-\pi, \pi]^2$ is completely mapped to $S_{n,m}$, $U_T$ must intersect one or more of the edges of $[-\pi, \pi]^2$. Hence there exists $u_0$ or $v_0$ such that either $S_{n,m}(u_0, -\pi) \neq S_{n,m}(u_0, \pi)$ or $S_{n,m}(-\pi, v_0) \neq S_{n,m}(\pi, v_0)$. But since $S_{n,m}(u, v) = \sum_{j=0}^{2n} \sum_{k=0}^{2m} d_{jk} B_j^n(u) B_k^m(v)$ where $B_j$'s are cyclic bases, $S_{n,m}(u, -\pi) = S_{n,m}(u, \pi)$ and $S_{n,m}(-\pi, v) = S_{n,m}(\pi, v)$ for all $u \in [-\pi, \pi]$ and $v \in [-\pi, \pi]$ which contradicts the supposition. ■

### 2.4. Model for the Control Points

Let $T_{2n+1,2m+1}(\mathbb{R}^p)$ denote the space of tensors of order $(2n+1) \times (2m+1) \times p$. Define $D^{n,m} = [d_{jk}]_{j=0,k=0}^{2m,2n}$. Clearly $D^{n,m} \in T_{2n+1,2m+1}(\mathbb{R}^3)$ for all $m \geq 1, n \geq 1$. Róth et al. (2009) remarked that although the control points have a global effect on the shape, this influence dramatically decreases on further parts of the surface, especially for higher value of $n$ and $m$. They provide several test examples to show that the decrease of the influence is fast. This observation is the key to the choice of sparsity favoring priors for $D^{n,m}$.

Because the elements of $D^{n,m}$ are expected to have an increasingly localized influence on the shape of the surface $S(u, v)$ as the index on the control points increases, we choose a shrinkage prior that favors smaller values for $d_{jk}$ as $n$ and $m$ increases. Here we use a double shrinkage prior to facilitate a sparseness of the tensors $D^{n,m}$.

$$d_{jk} \sim \mathrm{N}_3(0, \phi_{jk}^{-1} I_3),\ \phi_{jk} = \tau_j \xi_k,\ \tau_j \sim \mathrm{Ga}(\gamma_n, \beta), \xi_k \sim \mathrm{Ga}(\gamma_m, \beta), \tag{5}$$

where $\gamma_n$ is an increasing sequence of positive numbers.

The prior for $S$ induced from (1), (4) and (5), denoted $S \sim \Pi_{S^{n,m}}$, is defined conditionally on $n$ and $m$. If $n$ and $m$ are chosen to be too small, the prior $\Pi_{S^{n,m}}$ will not support a sizable subset of closed smooth surfaces. As an alternative to choosing $n$ and $m$ to be extremely large or even infinite to obtain large support, we propose to choose a prior for $n$ and $m$, which allows one to adaptively learn and model average over the unknown dimensions of the control point tensor $D^{n,m}$. Let $(n,m) \sim \Pi_{n,m}$ denote this prior, with $\Pi_{n,m}$ a distribution over $\{1, \ldots, \infty\}^2$, such as independent truncated Poisson distributions, and let $S \sim \Pi_S$ denote the resulting prior for $S$ marginalizing out $n$ and $m$. This approach is related to the literature on Bayesian adaptive splines (Denison et al., 1998), though we will bypass the need to implement the standard reversible jump Markov chain Monte Carlo and describe a computationally efficient approach in §3.

## 2.5. Prior Realizations

Let $\mathbb{T}^2$ denote the 2-dimensional torus represented by the square $[-\pi, \pi]^2$. Since $B_j^n(u) \geq 0, j = 0, \ldots, 2n, u \in [-\pi, \pi]$ and $\sum_{j=0}^{2n} B_j^n(u) = 1$, the closed surface $S_{n,m}(u,v) = \sum_{j=0}^{2n} \sum_{k=0}^{2m} d_{jk} B_j^n(u) B_k^m(v), (u,v) \in \mathbb{T}^2$ lies in the convex-hull of its control points $D^{n,m}$. We can achieve a variety of closed surfaces through specific choices of the control points as shown below in Fig. 2.5. The variety of shapes generated increases

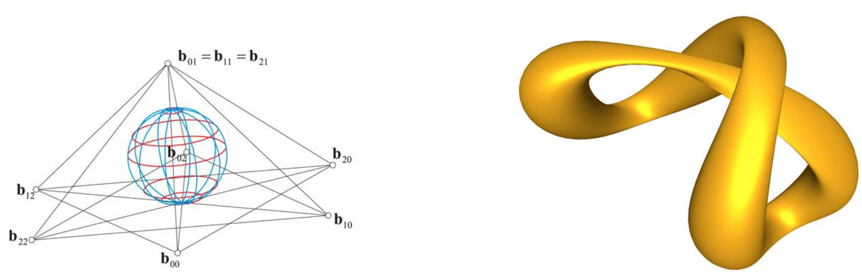


(a) A sphere with its control points (b) A closed surface with $n = 7$, $m = 9$

Figure 2: (a) A sphere with its control points (b) A closed surface with $n = 7$, $m = 9$. This figure is reproduced from Róth et al. (2009).

with increase in $n$ and $m$, the indices of the basis, which is shown in Fig. 2.5. Figure 2.5 also demonstrates that the influence of the control points is increasingly localized for large values of $n$ and $m$.

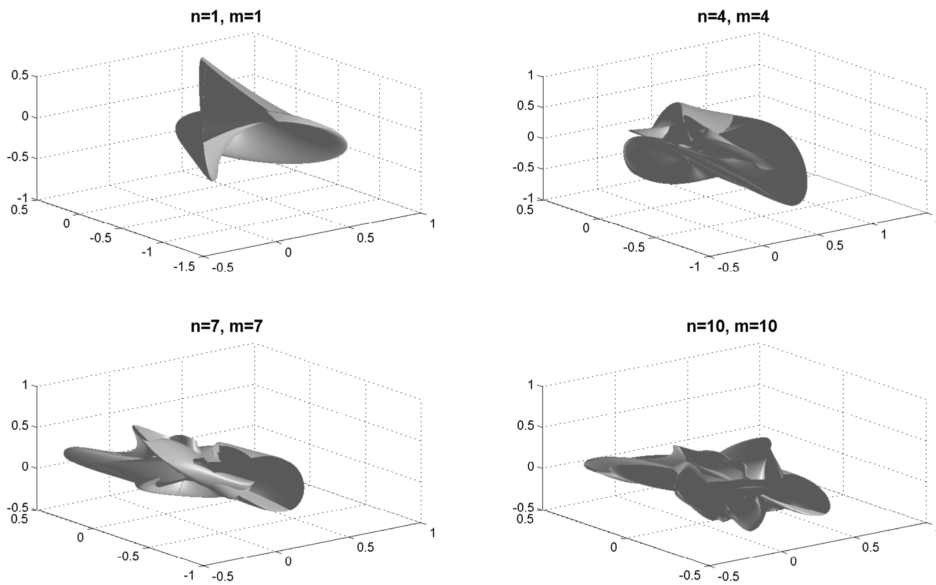


Figure 3: Prior realizations with increasing $n$ and $m$

## 3. Support of the Prior and Posterior Convergence Rates

### 3.1. General Notations

The supremum and $L_1$-norm are denoted by $||\cdot||_\infty$ and $||\cdot||_1$, respectively. We let $||\cdot||_{p,\nu}$ denote the norm of $L_p(\nu)$, the space of measurable functions with $\nu$-integrable $p$th absolute power. The notation $C(\mathcal{X})$ is used for the space of continuous functions $f : \mathcal{X} \to \mathbb{R}$ endowed with the uniform norm. For $\alpha > 0$ , we let $C^\alpha(\mathcal{X})$ denote the Hölder space of order $\alpha$, consisting of the functions $f \in C(\mathcal{X})$ that have $\lfloor \alpha \rfloor$ continuous derivatives with the $\lfloor \alpha \rfloor$th derivative $f^{\lfloor \alpha \rfloor}$ being Lipschitz continuous of order $\alpha - \lfloor \alpha \rfloor$. The $\epsilon$-covering number $N(\epsilon, T, d_M)$ of a semi-metric space $T$ relative to the semi-metric $d_M$ is the minimal number of balls of radius $\epsilon$ needed to cover $T$. The logarithm of the covering number is referred to as the entropy. $\oint$ stands for the complex line integral. We write "$\precsim$" for inequality up to a constant multiple and $\{a_{(1)}, a_{(2)}, \dots, a_{(n)}\}$ to denote the order statistics of the set $\{a_i : a_i \in \mathbb{R}, i = 1, \dots, n\}$.

### 3.2. Support

Let the Hölder class of bivariate periodic functions on $\mathbb{T}^2$ of order $\alpha$ be denoted by $C^\alpha(\mathbb{T}^2)$. Define a class of closed parametric surfaces $\mathcal{S}_\mathcal{C}(\alpha_1, \alpha_2, \alpha_3)$ having different smoothness along different coordinates as

$$\mathcal{S}_\mathcal{C}(\alpha_1, \alpha_2, \alpha_3) := \{S = (S^1, S^2, S^3) : \mathbb{T}^2 \to \mathbb{R}^3, S^i \in C^{\alpha_i}(\mathbb{T}^2), i = 1, 2, 3\}.$$

From Lemma 5, $\mathcal{S}_{\mathcal{C}}(\alpha_1, \alpha_2, \alpha_3)$ is contained in the set of all closed $\mathbb{T}^2 \to \mathbb{R}^3$ parametric surfaces. For fixed $n$ and $m$, define the stochastic process $S \sim \Pi_{S^{n,m}}$. To characterize the support of our prior, we first recall the definition of the reproducing kernel Hilbert space (RKHS) of a multivariate Gaussian process prior. van der Vaart and van Zanten (2008) review facts that are relevant to the present setting. A Borel measurable random element $W$ with values in a separable Banach space $(\mathbb{B}, ||\cdot||)$ is called Gaussian if the random variable $b^*W$ is normally distributed for any element $b^* \in \mathbb{B}^*$, the dual space of $\mathbb{B}$. In our case, the Banach space $\mathbb{B}$ is $C(\mathbb{T}^2;\mathbb{R}^3)$, the space of continuous functions from $\mathbb{T}^2$ to $\mathbb{R}^3$. The RKHS $\mathbb{H}$ attached to a zero-mean Gaussian process $W$ is defined as the completion of the range $M\mathbb{B}^*$ of the map $M : \mathbb{B}^* \to \mathbb{B}$ defined by $Mb^* = \mathrm{E}Wb^*(W)$ relative to the inner product

$$\langle Mb_1^*, Mb_2^* \rangle_{\mathbb{H}} = \mathrm{E}b_1^*(W)b_2^*(W).$$

The following lemma describes the RKHS of the Gaussian process $\Pi_{S^{n,m}}$ given $\{\phi_{jk}, j = 0,\ldots,2n, k = 0,\ldots,2m\}$ defined in (5).

**Lemma 6** *Given $\{\phi_{jk}, j = 0,\ldots,2n, k = 0,\ldots,2m\}$, the RKHS $\mathbb{H}^{n,m}$ of $\Pi_{S^{n,m}}$ consists of all functions $h : \mathbb{T}^2 \to \mathbb{R}^3$ of the form*

$$h(u, v) = \sum_{j=0}^{2n}\sum_{k=0}^{2m} c_{jk} B_j^n(u) B_k^m(v),$$

*where the weights $c_{jk}$ range over $\mathbb{R}^3$. The RKHS norm is given by*

$$||h||^2_{\mathbb{H}^{n,m}} = \sum_{j=0}^{2n}\sum_{k=0}^{2m} ||c_{jk}||^2 \phi_{jk}.$$

The following theorem describes how well an arbitrary closed parametric surface $S_0 \in \mathcal{S}_{\mathcal{C}}(\alpha_1, \alpha_2, \alpha_3)$ can be approximated by the elements of $\mathbb{H}^{n,m}$ for each $n$ and $m$ given $\{\phi_{jk}, j = 0,\ldots,2n, k = 0,\ldots,2m\}$.

**Theorem 7** *For any fixed $S_0 \in \mathcal{S}_{\mathcal{C}}(\alpha_1, \alpha_2, \alpha_3)$, there exists $h \in \mathbb{H}^{n,m}$ with $||h||^2_{\mathbb{H}^{n,m}} \leq K_1 \sum_{j=0}^{2n}\sum_{k=0}^{2m} \phi_{jk}$ such that*

$$||S_0 - h||_\infty \leq K_2 (n \wedge m)^{-\alpha_{(1)}} \log n \log m$$

*for some constants $K_1, K_2 > 0$ independent of $n$ and $m$.*

### 3.3. Rate of Convergence of the Posterior

The parameter space is $C(\mathbb{T}^2;\mathbb{R}^3) \times [0,\infty) \times [-\pi,\pi]^2$ and $\Pi_S \times \Pi_\sigma \times \Pi_{[-\pi,\pi]^2}$ is the prior on $C(\mathbb{T}^2;\mathbb{R}^3) \times [0,\infty) \times [-\pi,\pi]^2$ where $\Pi_\sigma$ denotes a general prior for $\sigma$ which is compactly supported on $[0, L]$ for some $L > 0$. Assume that the density of $\Pi_\sigma$ with respect to the Lebesgue measure on the compact interval is bounded away from zero and $\Pi_{[-\pi,\pi]^2}$ has a density with respect to Lebesgue measure on $[-\pi,\pi]^2$ which is nowhere zero. The inverse gamma prior truncated to the interval $[0, L]$ provides an example.

**Definition 8** *For a given sequence $\epsilon_N \downarrow 0$, the posterior is said to contract around the true parameter value $(S_0, \sigma_0) \in C(\mathbb{T}^2; \mathbb{R}^3) \times [0, \infty)$ at a rate $\epsilon_N$ if for $M$ sufficiently large,*

$$\Pi_{S_0,\sigma_0}\left[(S,\sigma) : \int_{[-\pi,\pi]^2} ||S(u,v) - S_0(u,v)||^2 d\Pi_{[-\pi,\pi]^2}(u,v) + |\sigma - \sigma_0|^2 > M\epsilon_N^2 \,\middle|\, \{p_i, (u_i, v_i)\}_{i=1}^N\right] \to 0 \text{ as } N \to \infty.$$

**Theorem 9** *If $(S_0, \sigma_0) \in \mathcal{S}_{\mathcal{C}}(\alpha_1, \alpha_2, \alpha_3) \times [0, L]$, $\Pi_S \times \Pi_\sigma \times \Pi_{[-\pi,\pi]^2}$ is the prior on $C(\mathbb{T}^2; \mathbb{R}^3) \times [0, \infty) \times [-\pi, \pi]^2$ as defined above with $\gamma_n = O(\log n)^3$ and $\exp\{-(nr + ms)\} \leq \Pi_{n,m} \leq (nm)^{-3}, n, m \geq 1$ for some $r, s > 0$, then the posterior contracts around $(S_0, \sigma_0)$ at the rate $\epsilon_N = N^{-\frac{\alpha_{(1)}}{2\alpha_{(1)}+2}} \log^t N$, where $t$ is a known constant.*

The proofs of Lemma 6, Theorem 7 and Theorem 9 are deferred to the Appendix. The assumption on $\Pi_{n,m}$ ensures that the prior probability is not too small on smaller values of $n$ and $m$ so that the prior favors relatively simple representations of the surface. The assumption is satisfied by a product of independent Poisson distributions. Also the shape parameter of the Gamma distribution for $\tau_j$ and $\xi_k$ should be increased depending on the values of $n$ and $m$ to guarantee an optimal rate of convergence. The increase in shape parameter with $n$ and $m$ corresponds to a greater shrinkage of the higher indexed control points. To estimate a real valued $d$-variate function in $C^\alpha(\mathcal{X})$, the minimax optimal rate of convergence is $n^{-\alpha/(2\alpha+d)}$. One can anticipate that for vector valued functions with smoothness $\alpha_j, j = 1, 2, 3$ in the coordinates, with the loss function defined by the sum of the individual loss across the coordinates, the rate of convergence cannot be improved beyond $n^{-\alpha_{(1)}/(2\alpha_{(1)}+d)}$. Theorem 9 ensures that the posterior will converge to the true surface at this rate which is offset slightly by a logarithmic factor as expected for Bayesian procedures (de Jonge and van Zanten, 2010; van der Vaart and van Zanten, 2009).

## 4. Posterior Computation

Since fully Bayes posterior updates of all the unknown parameters will require a computationally intensive Metropolis-Hastings step to update the $\{(u_i, v_i), i = 1, \ldots, N\}$ within the Gibbs sampler, we consider a simpler two-stage estimation. In the first stage, we estimate $\{(u_i, v_i), i = 1, \ldots, N\}$, a procedure popularly termed as *parameterization*. In the second stage, we plug the values of $\{(u_i, v_i), i = 1, \ldots, N\}$ obtained in the first stage and perform Gibbs sampling to update the remaining parameters as described in §4.2 and §4.3.

### 4.1. Empirical Bayes Estimation of $\{(u_i, v_i), i = 1, \ldots, N\}$

We formally define parameterization below.

**Definition 10** *Parameterization is an algorithm to find the coordinate $(u_i, v_i)$ corresponding to the observed data point $p_i$ for each $i = 1, \ldots, N$ such that there exists a parametric surface $S$ so that $p_i$ is regarded as an error-prone realization of $S(u_i, v_i), i = 1, \ldots, N$. The coordinate chart $\{(u_i, v_i), i = 1, \ldots, N\}$ is alternatively termed as the associated parameter values.*

Since we intend to fit a parametric surface, we have to find the coordinate chart $\{(u_i, v_i) \in [a, b]^2\}$ corresponding to the points $\{p_i \in \mathbb{R}^3, i = 1, \ldots, N\}$. Closed surfaces can be achieved by parameterizations on the sphere or the torus. The parameterizations are typically estimated from the data by, for example, projecting the points $\{p_i\}$ onto a suitably chosen plane. Spherical harmonics were originally used as a type of parametric surface representation for radial or steller surfaces $S(u, v), 0 < u < 2\pi, 0 < v < \pi$ (Brechbühler et al., 1995; Shen and Makedon, 2006). The idea is to project the data on the sphere by constrained optimization and then recover the surface by fitting $S(u, v)$ to $p_i, i = 1, \ldots, N$. Parameterization with the torus topology has the advantage of encompassing a wider range of closed surfaces compared to spherical harmonic functions which can only model sphere-like or convex surfaces. We use the relational perspective map developed by Li (2004) to project the 3-d point cloud onto a torus and then scale down to $[-\pi, \pi]^2$. The relational perspective mapping is a multidimensional scaling algorithm with topological constraints. It preserves the neighborhood property of the 3d points $p_i$ in the projected points $(u_i, v_i)$ by minimizing an energy function $\sum_{1 \le i < j < N} (\delta^1_{ij} - \delta^2_{ij})^2 / \delta^2_{ij}$ where $\delta^1_{ij} = ||p_i - p_j||$ and $\delta^2_{ij} = ||(u_i, v_i) - (u_j, v_j)||$ subject to the constraint that the points $(u_i, v_i)$ lies on a torus. Applying the relational perspective map to the point cloud in Fig. 1, we obtain the points in the $[-\pi, \pi]^2$ square shown in Fig. 4.1.

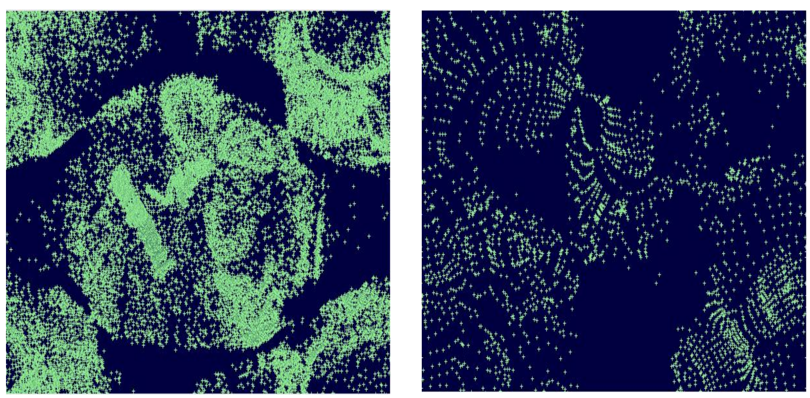

Figure 4: Parameterization of the human skull and the Beethoven data

### 4.2. Gibbs Sampler for a Fixed Truncation Level and $\{(u_i, v_i), i = 1, \ldots, N\}$

For a fixed $n$ and $m$, the full conditional distributions of all the unknown variables are conjugate and we can do Gibbs sampling. The sampler cycles through the following steps. *Step 1.* Define $X$ to be the $N \times (2n+1)(2m+1)$ matrix with rows $\{B^n_0(u_i), B^n_1(u_i), \ldots, B^n_{2n}(u_i)\} \otimes \{B^m_0(v_i), B^m_1(v_i), \ldots, B^m_{2m}(v_i)\}, i = 1, \ldots, N$. Also let $D$ be the $(2n+1)(2m+1) \times 3$ coefficient matrix with rows $d^{\mathrm{T}}_{jk}$, $j = 0, 1, \ldots, 2n, k = 0, 1, \ldots, 2m$. Recall that the density of a matrix-normal random variable $Z \sim \mathrm{MN}(M, \Omega, \Sigma)$ with mean $M$ having dimension $n \times p$ is given by

$$f(z \mid M, \Omega, \Sigma) \propto \exp[-0{\cdot}5\mathrm{tr}\{\Omega^{-1}(z - M)^{\mathrm{T}}\Sigma^{-1}(z - M)\}],$$

for positive definite matrices $\Omega$ and $\Sigma$ of order $p \times p$ and $n \times n$. Then

$$D \mid - \quad \sim \quad \mathrm{MN}_{(2n+1)(2m+1)\times 3}\left[(1/\sigma^2)X^{\mathrm{T}}P, I_3, \{(1/\sigma^2)X^{\mathrm{T}}X + \Lambda^{-1}\}^{-1}\right],$$

$$\mathrm{vec}(D) \mid - \quad \sim \quad \mathrm{N}_{3(2n+1)(2m+1)}\Big[\mathrm{vec}\{(1/\sigma^2)X^{\mathrm{T}}P\}, I_3 \otimes \{(1/\sigma^2)X^{\mathrm{T}}X + \Lambda^{-1}\}^{-1}\Big].$$

Here $\Lambda^{-1} = \mathrm{diag}\{\tau_j \xi_k, j = 0, \ldots, 2n, k = 0, \ldots, 2m\}$.
*Step 2.*

$$\sigma^{-2} \mid - \sim \mathrm{Ga}\Big(a_\sigma + 3N/2, b_\sigma + 0{\cdot}5 \sum_{i=1}^{N} ||p_i - S(u_i, v_i)||^2\Big).$$

*Step 3.* For $j = 0, \ldots, 2n$ and $k = 0, \ldots, 2m$,

$$\tau_j \mid - \sim \mathrm{Ga}\Big\{\gamma_n + 3(2m+1)/2, \beta + 0{\cdot}5 \sum_{k=0}^{2m} \xi_k ||d_{jk}||^2\Big\}.$$

$$\xi_k \mid - \sim \mathrm{Ga}\Big\{\gamma_m + 3(2n+1)/2, \beta + 0{\cdot}5 \sum_{j=0}^{2n} \tau_j ||d_{jk}||^2\Big\}.$$

### 4.3. Posterior Sampling of $n$ and $m$

The conditional likelihood of $n, m, \{(d_{jk}, \phi_{jk}), j = 0, \ldots, 2n, k = 0, \ldots, 2m\}$ given $\{p_i, (u_i, v_i), i = 1, \ldots, N\}$ is proportional to

$$\exp\Big( - \frac{1}{2\sigma^2} \sum_{i=1}^{N} ||p_i - S_{n,m}(u_i, v_i)||^2\Big)\Pi_{n,m} \prod_{j=0}^{2n} \prod_{k=0}^{2m} p(d_{jk} \mid \phi_{jk}) p(\phi_{jk}).$$

In this case, rather than proposing an entirely new parameter vector, the form of reversible jump Markov chain Monte Carlo for $n$ and $m$ becomes relatively straightforward. The common parameters $\sigma^{-2}$ and $\{d_{jk}, j = 0, \ldots, 2n, k = 0, \ldots, 2m\}$ as the order of the model changes are updated using a within model Gibbs move as in §4.2. Consider a proposal $q(n, m \mid n_0, m_0) = q(n \mid n_0) q(m \mid m_0)$ with $q(1 \mid 0) = 1$ and $q(k' \mid k) = 1/2$ for all $|k - k'| = 1$. Suppose the chain is at $(n_0, m_0)$ and a proposal is made to go to state $(n_0 + 1, m_0 + 1)$, we employ a step-wise sampler as in Godsill (2001). We sample $(d'_{2n_0+1,2m_0+1}, \phi'_{2n_0+1,2m_0+1})$ and $(d'_{2n_0+2,2m_0+2}, \phi'_{2n_0+2,2m_0+2})$ from a kernel $ker(d_{jk}, \phi_{jk})$ and the move is accepted with probability $\min\{1, \alpha\}$, where

$$\alpha = \frac{\exp\big( - \frac{1}{2\sigma^2} \sum_{i=1}^{N} ||p_i - S_{n_0+1,m_0+1}(u_i, v_i)||^2\big)\Pi_{n_0+1,m_0+1}}{\exp\big( - \frac{1}{2\sigma^2} \sum_{i=1}^{N} ||p_i - S_{n_0,m_0}(u_i, v_i)||^2\big)\Pi_{n_0,m_0}} \times \frac{q(n_0 + 1, m_0 + 1 \mid n_0, m_0)}{q(n_0, m_0 \mid n_0 + 1, m_0 + 1) \prod_{j=1}^{2} ker(d'_{2n_0+j,2m_0+j}, \phi'_{2n_0+j,2m_0+j})}.$$

We take $ker(d_{jk}, \phi_{jk}) = p(d_{jk}, \phi_{jk})$. The proposal probabilities for the moves $(n_0, m_0) \to (n_0, m_0 \pm 1)$, $(n_0, m_0) \to (n_0 \pm 1, m_0)$ and $(n_0, m_0) \to (n_0 \pm 1, m_0 \pm 1)$ can be derived similarly. The shrinkage prior on the $\phi_{jk}$'s gives rise to highly efficient moves which converge to the appropriate values of $n$ and $m$ rapidly in most cases we have observed.

## 5. Applications

We analyzed the skull and Beethoven data shown in Fig. 1 using our proposed method. As all reasonable methods will do a good job at surface estimation based on a large number of points located very close to the surface of interest, we simulated different levels of sparse and noisy data by sampling a subset of the points in the original data sets and adding different levels of Gaussian measurement errors. In many other applications, sparse and noisy data are routinely collected but focusing on two dense, low measurement error data sets allows careful study of the impact of sample size and measurement error on the performance of our proposed Bayesian approach relative to the state-of-the-art Crust algorithm.

First we reconstruct the surface from non-noisy sparse data by taking random subsamples of 390 points from the skull and Beethoven point clouds. Refer to the Appendix for Figs A - A. The results for Crust are shown in Fig. A, while the results for the posterior mean surface obtained from our Bayesian approach are shown in Fig. 6. In each case, we generated 5000 samples and discarded the first 2000 as burn-in. Convergence was monitored using trace plots of the deviance as well as several parameters. Also we get essentially identical posterior modes of $n$ and $m$ with different starting points and moderate changes to hyperparameters.

In many applications, the features of the data acquisition device can dictate the amount of noise incorporated. Choosing an informative prior for the noise variance can help in the ability to pick up local features. The hyperparameters in the priors for $\tau_j$ and $\xi_k$ play a key role in controlling the smoothness of the surface. An increase in $\gamma_n$ corresponds to a decrease in the values of $\tau_j$ and $\xi_k$ leading to over-smoothing. Estimation of noise variance and the surface is robust to moderate changes in hyperparameters as the sample size increases.

Our method performs closely to Crust for non-noisy data. As we add Gaussian noise to the points, the performance of Crust deteriorates (Fig. A) while the tensor product surface (Fig. A) is quite robust to the addition of noise as it takes into account the uncertainty in estimating the surface. In Fig. A, we notice some parts from the skull and the Beethoven's head jutting out owing to poor characterization of the noise.

To compare the performance of our method with existing competitors, we compute the Hausdorff distance between the true surface and the fitted surface as described below. Let $S_1$ and $S_2$ be two manifolds embedded in $\mathbb{R}^3$. Then the Hausdorff distance is defined by

$$h_D(S_1, S_2) = \max\left\{ \sup_{x \in S_1} \inf_{y \in S_2} d(x,y), \sup_{x \in S_2} \inf_{y \in S_1} d(x,y) \right\}$$

where $d$ is any distance in $\mathbb{R}^3$. It can be shown that $h_D(S_1, S_2) = 0$ if and only if $S_1$ and $S_2$ have the same closure. For the tensor product approach we estimate $h_D(S, \hat{S})$ by $\max\{\sup_i \inf_j d(p_i, \hat{p}_j), \sup_j \inf_i d(p_i, \hat{p}_j)\}$ where $\{\hat{p}_i, i = 1, \ldots, N\}$ is a Bayes estimate of $\{p_i, i = 1, \ldots, N\}$ where $d$ is the standard Euclidean distance. For the Crust algorithm, we estimate $h_D(S, \hat{S})$ by $\max\{\sup_i \inf_j d(p_i, t_j), \sup_j \inf_i d(p_i, t_j)\}$ where $\{t_i : i = 1, \ldots, M\}$ is a dense grid of points on the resulting simplicial surface.

We summarize the performances of the Crust algorithm and the tensor product approach in Table 1 for a variety of choices of the sample size and noise variance ($\sigma^2$). We observe that for non-noisy data Crust performs closely and slightly better than the tensor-product surface for large sample sizes while the tensor product outperforms the Crust as the noise variance

Table 1: Hausdorff distance between true and fitted surface using tensor product method and Crust

| | Skull | | | Beethoven | | |
|---|---|---|---|---|---|---|
| $\sigma$ | N=390 | N=690 | N=990 | N=390 | N=690 | N=990 |
| 0·05 | (2·123, 2·045) | (2·008, 1·971) | (1·981, 1·791) | (1·528, 1·557) | (1·510, 1·527) | (1·411,1·397) |
| 0·1 | (2·561, 2·671) | (2·345, 2·682) | (2·311, 2·677) | (1·589, 1·679) | (1·524, 1·560) | (1·579, 1·730) |
| 0·2 | (2·711, 3·134) | (2·697, 3·225) | (2·523, 3·435) | (1·812, 2·146) | (1·796 ,1·874) | (1·657, 2·334) |

Table 2: Posterior summaries of $\sigma$ and $n, m$ (posterior mean of $\sigma$, 95% credible intervals for $\sigma$, posterior mode of $(n, m)$)

| $\sigma$ | N=390 | N=690 | N=990 |
|---|---|---|---|
| | | Skull | |
| 0·05 | 0·075, [0·065, 0·093], (3,4) | 0·064, [0·056, 0·077], (4,4) | 0·056, [0·047, 0·062], (4,4) |
| 0·1 | 0·194, [0·124, 0·265], (4,4) | 0·154 [0·096, 0·213], (4,4) | 0·120, [0·081, 0·156], (3,4) |
| 0·2 | 0·220, [0·127, 0·314], (3,4) | 0·210 [0·136, 0·279], (3,4) | 0·196 [0·139, 0·253], (3,4) |
| | | Beethoven | |
| 0·05 | 0·090, [0·081 0·109], (5,6) | 0·061, [0·041, 0·081], (6,6) | 0·054, [0·039, 0·067], (6,7) |
| 0·1 | 0·220, [0·191, 0·261], (5,6) | 0·171,[0·143, 0·191], (5,6) | 0·167, [0·091, 0·159], (6,6) |
| 0·2 | 0·228, [0·166, 0·291], (5,6) | 0·214, [0·161, 0·267], (5,6) | 0·203 [0·161, 0·246], (5,6) |

increases. As the sample size increases, the tensor product surface fit becomes better even when the noise variance is large. However, the performance of the Crust improves with sample size only when the noise variance is very small. Posterior summaries of the noise variance and the basis function truncation levels $n$ and $m$ are provided in Table 2. The noise variance is not well-estimated for small sample sizes and smaller value of the true noise variance. However, estimation becomes better for larger sample sizes consistent with the posterior convergence results. Also, one can estimate larger variances well compared to smaller ones for reasons discussed earlier. As the sample size increases, the posterior mode of $(n, m)$ tend to increase slightly when the noise variance is small in order to capture local features. When the noise variance is large, the global features dominate and the posterior modes of $n$ and $m$ remain constant at the smaller values.

## 6. Discussion

This article develops a novel Bayesian hierarchical model for a closed surface, allowing full posterior inferences via an efficient Markov chain Monte Carlo algorithm. Consistent with our theory results on optimal rates of posterior contraction, we find that the methodology does a good job in reconstructing a closed surface from sparse and noisy 3d point cloud data yielding improved performance over state-of-the-art computer science algorithms. Although modern sensing technology, such as computed tomography or magnetic resonance imaging, enables us to make detailed scans of complex objects generating point cloud data consisting of millions of points, the data acquired is usually distorted by noise arising out of various physical measurement processes and limitations of the acquisition technology. Most of these points are typically discarded after taking into account acquisition effects leading to a sparse noisy point cloud. The resolution specifics of these acquisition devices provide information on the magnitude of the measurement error variance. A major advantage of the proposed model is that the Markov chain Monte Carlo algorithm is quite simple and easy to implement rapidly which makes it particularly easy to include generalizations (e.g., to heavy-tailed residual densities, background clutter, etc). An appealing feature of our Bayesian approach is that we obtain a full posterior for the surface allowing uncertainty. Visualizing this uncertainty is an interesting challenge for future research, but one can produce interior and exterior pointwise 95% credible surfaces and even movies of surface realizations from the posterior. In addition, when there is interest in surface features, such as the interior volume, surface area, or the number of holes, one can obtain posterior summaries of the feature of interest.

Our proposed approach represents an initial step in a line of research related to Bayesian modeling of 3-d closed surfaces. There are several important next steps. The use of parameterization domains that are closed surfaces of arbitrary genus would require carefully chosen basis functions. It is also commonly the case that each subject has their own surface and interest focuses on modeling a collection of dependent surfaces across subjects, while incorporating subject-specific predictors, using the surface to predict a response variable, and testing differences in distributions of surfaces between groups. In such settings, it is necessary to align the surfaces for the different subjects, which can potentially be accomplished in a Bayesian probabilistic framework. Another ongoing problem relates to surfaces that change dynamically over time within a subject. In addition, it is common for the data to not consist simply of a 3-d point cloud but instead to have pixelated data in which the surface(s) of interest are embedded in an blurry image containing other objects.

As in other functional data modeling settings, the smoothness and local features of the surfaces being estimated can be somewhat sensitive to the basis functions being used. We have focused on tensor products of truncated Fourier series, which lead to obtain rates of posterior contraction and have good practical performance in reconstructing infinitely smooth surfaces that have cross sections that are closed curves. There are settings in which the objects being modeled may have interesting local features, such as spikes, that may be smoothed out with our proposed bases and shrinkage priors in the absence of abundant data.

## Acknowledgement

This research was supported by a grant from the National Institute of Environmental Health Sciences (NIEHS) of the National Institutes of Health (NIH).

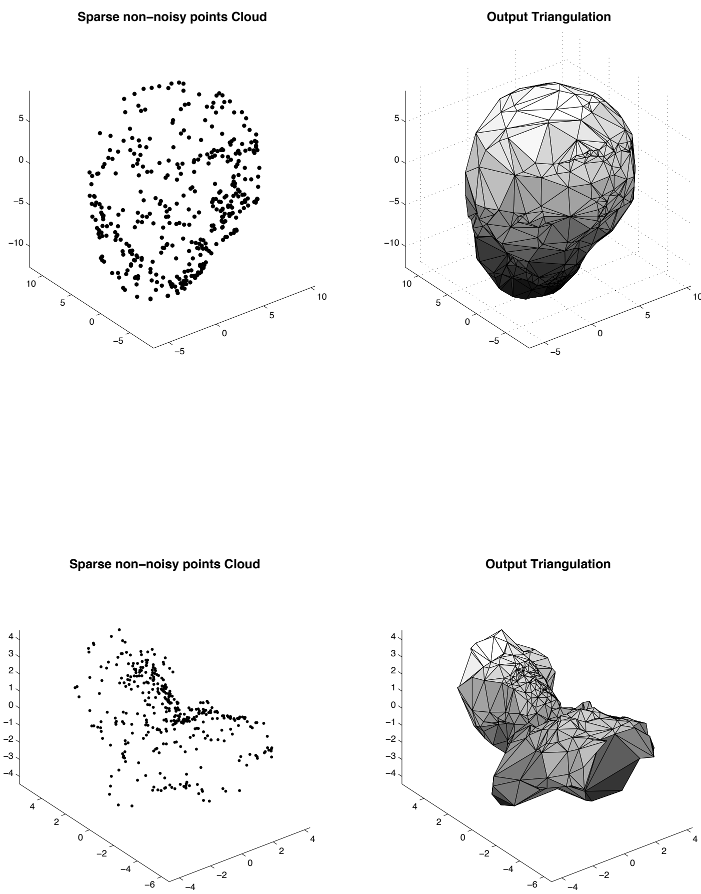


Figure 5: Output triangulation from crust algorithm on a sparse (390 points) non-noisy point cloud

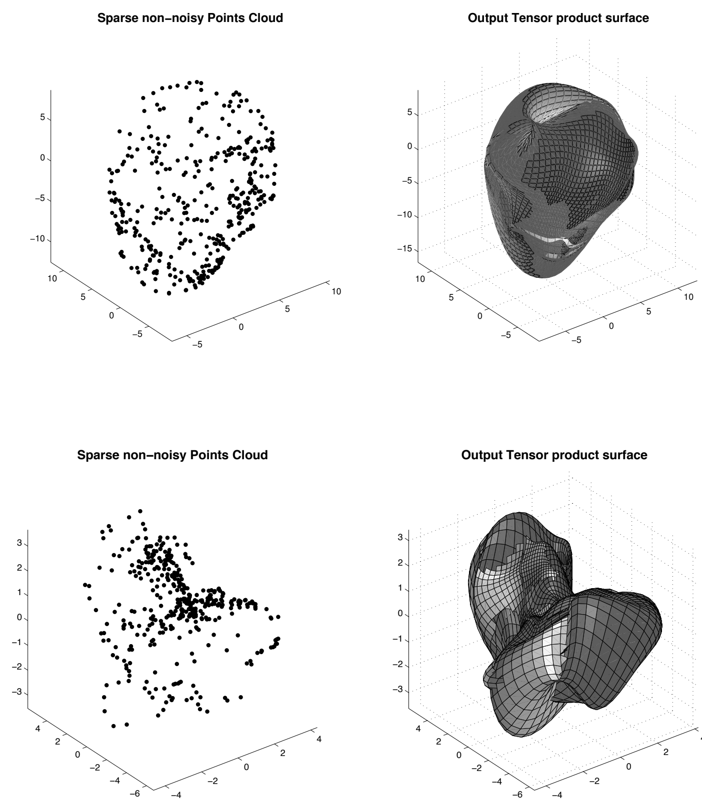


Figure 6: Output tensor product surface on a sparse (390 points) non-noisy point cloud

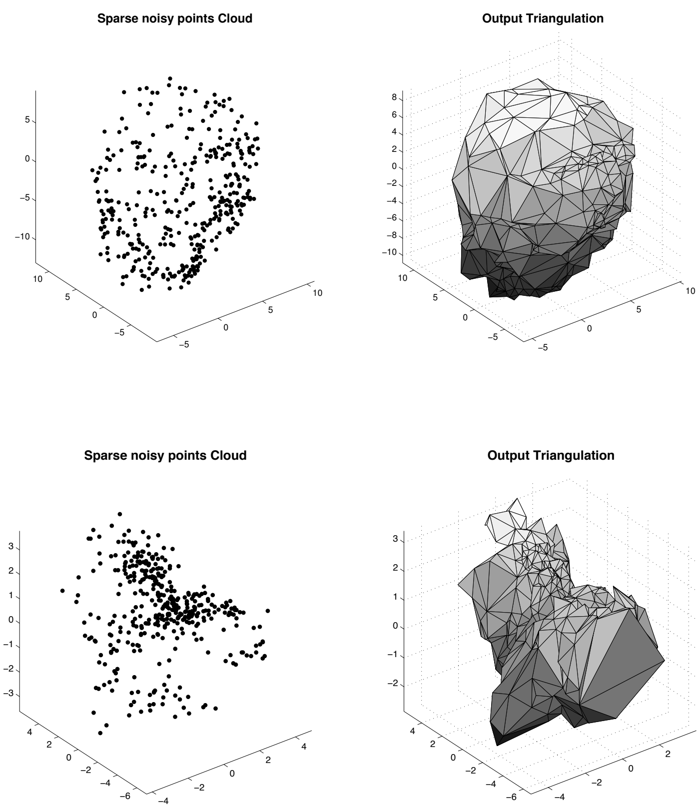


Figure 7: Output triangulation from crust algorithm on a sparse (390 points) noisy (std=0.2) point cloud

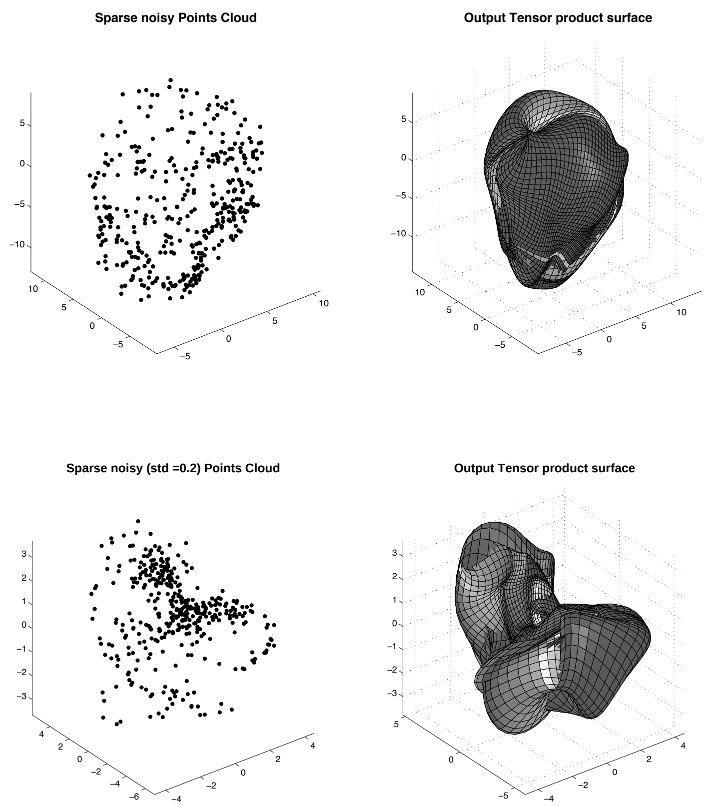


Figure 8: Output tensor product surface on a sparse (390 points) noisy (std=0.2) point cloud

## Appendix A.

*Proof of Lemma 6.* The Gaussian process prior $\Pi_{S^{n,m}}$ given $\{\phi_{jk}, j = 0,\ldots,2n, k = 0,\ldots,2m\}$ has the following representation.

$$S^{n,m}(u,v) = \sum_{j=0}^{2n}\sum_{k=0}^{2m} d_{jk}B_j^n(u)B_k^m(v),\ d_{jk} \sim \mathrm{N}_3(0, \phi_{jk}^{-1}I_3),\ (u,v) \in \mathbb{T}^2.$$

To characterize the RKHS of $S^{n,m}(u,v)$, we need the following generalization of Theorem 4.2 of van der Vaart and van Zanten (2008) to the multivariate case.

**Proposition 11** *Let $(h_i)$ be a sequence of elements in a separable Banach space $\mathbb{B}$ such that $\sum_{i=1}^{\infty} w_i h_i = 0$ for a sequence $w \in \ell_2(\mathbb{R}^3)$, where the convergence is in $\mathbb{B}$, implying that $w = 0$. Let $Z_i = (Z_{i1}, Z_{i2}, Z_{i3})^{\mathrm{T}} \sim N_3(0, I_3)$, and assume that the series $W = \sum_{i=1}^{\infty} Z_i h_i$ converges almost surely in $\mathbb{B}^3$. Then the RKHS of $W$ as a map in $\mathbb{B}^3$ is given by $\mathbb{H} = \{\sum_{i=1}^{\infty} w_i h_i : w \in \ell_2(\mathbb{R}^3)\}$ with squared norm $||\sum_{i=1}^{\infty} w_i h_i||_{\mathbb{H}}^2 = \sum_{i=1}^{\infty} ||w_i||^2$.*

**Proof** The almost sure convergence of the series $W = \sum_{i=1}^{\infty} Z_i h_i \in \mathbb{B}^3$ implies almost sure convergence of the series $b^*W$ for any $b^* \in (\mathbb{B}^3)^*$. Now any $b^* \in (\mathbb{B}^3)^*$ can be written as $b^* = \alpha_1 b_1^* + \alpha_2 b_2^* + \alpha_3 b_3^*$ for $\alpha_i \in \mathbb{R}, b_i^* \in \mathbb{B}^*$. Hence $b^*W = \sum_{j=1}^{3} \alpha_j \sum_{i=1}^{\infty} Z_{ij} b_j^* h_i$. Since the partial sums of the last series are zero mean Gaussian, the series also converges in $L_2(\Omega, \mathcal{U}, \mathcal{P})$. Hence for $b^*, \underline{b}^* \in (\mathbb{B}^3)^*$,

$$\mathrm{E}b^*W\underline{b}^*W = \sum_{j=1}^{3} \alpha_j \underline{\alpha}_j \sum_{i=1}^{\infty} b_j^* h_i \underline{b}_j^* h_i.$$

For $w \in \ell_2(\mathbb{R}^3)$ and natural numbers $m < n$, by the Hahn-Banach theorem and the Cauchy-Schwartz inequality, we have

$$\begin{aligned} ||\sum_{m\le i\le n} w_i h_i||^2 &= \sup_{||b^*||\le 1} ||\sum_{j=1}^{3} \alpha_j \sum_{m\le i\le n}^{\infty} w_{ij} b_j^* h_i||^2 \\ &\le 3 \sup_{||b^*||\le 1} \sum_{j=1}^{3} \alpha_j^2 \sum_{m\le i\le n} w_{ij}^2 \sum_{m\le i\le n} (b_j^* h_i)^2 \\ &\le 3(\sum_{j=1}^{3}\sum_{m\le i\le n} w_{ij}^2) \sup_{||b^*||\le 1} \sum_{j=1}^{3} \alpha_j^2 \sum_{m\le i\le n} (b_j^* h_i)^2 \end{aligned}$$

As $m, n \to 0$, the first term on the far right converges to zero as $w \in \ell_2(\mathbb{R}^3)$. By the first paragraph the second factor is bounded by $\sup_{||b^*||\le 1} \mathrm{E}(b^*W)^2 \le \mathrm{E}||W||^2$. Hence the partial sums of the series $\sum_i w_i h_i$ form a Cauchy sequence in $\mathbb{B}^3$ and hence it converges.

Because $\sum_{i=1}^{\infty} (b_j^* h_i)^2$ was seen to converge for each $j = 1, 2, 3$, it follows that $\sum_{i=1}^{\infty} (b_j^* h_i) h_i$ converge in $\mathbb{B}$, and hence $\underline{b}^* \sum_{i=1}^{\infty} (\alpha_1 b_1^* h_i, \alpha_2 b_2^* h_i, \alpha_3 b_3^* h_i)^{\mathrm{T}} h_i = \sum_{j=1}^{3} \alpha_j \underline{\alpha}_j \sum_{i=1}^{\infty} b_j^* h_i \underline{b}_j^* h_i = \mathrm{E}b^*W\underline{b}^*W$, for any $\underline{b}^* \in (\mathbb{B}^3)^*$. This shows that $Mb^* = \sum_{i=1}^{\infty} (\alpha_1 b_1^* h_i, \alpha_2 b_2^* h_i, \alpha_3 b_3^* h_i)^{\mathrm{T}} h_i$ and the RKHS is not bigger than this space. Also $||Mb^*||_{\mathbb{H}}^2 = \sum_{j=1}^{3} \alpha_j^2 \sum_{i=1}^{\infty} (b_j^* h_i)^2$.

Thus the RKHS consists of elements $\sum_{i=1}^{\infty} w_i h_i = \sum_{i=1}^{\infty} w_i h_i$ where $w_i \in \ell_2(\mathbb{R}^3)$ and $||\sum_{i=1}^{\infty} w_i h_i||_{\mathbb{H}}^2 = \sum_{i=1}^{\infty} ||w_i||^2$.

The space would have been smaller than claimed if there existed $w \in \ell_2(\mathbb{R}^3)$ that is not in the closure of the linear span of the elements $(b^* h_i)$ of $\ell_2(\mathbb{R}^3)$ when $b^*$ ranges over $(\mathbb{B}^*)^3$. Without loss of generality, we can take this $w$ to be orthogonal to the later collection, i.e., $\sum_{j=1}^{3} \alpha_j \sum_i w_{ij} b_j^* h_i = 0$ for every $b^* \in (\mathbb{B}^*)^3$. This is equivalent to $\sum_i w_{ij} h_i = 0$ for $j = 1, 2, 3$ which implies $w = 0$. ■

Since $d_{jk} \sim \mathrm{N}_3(0, \phi_{jk}^{-1} I_3)$, $\Pi_{S^{n,m}}$ can be written as

$$S^{n,m}(u,v) = \sum_{j=0}^{2n} \sum_{k=0}^{2m} b_{jk}^* \phi_{jk}^{-1/2} B_j^n(u) B_k^m(v),$$

where $b_{jk}^* \sim \mathrm{N}_3(0, I_3)$. Hence $\mathbb{H}^{n,m}$ consists of $h : \mathbb{T}^2 \to \mathbb{R}^3$ such that

$$h(u,v) = \sum_{j=0}^{2n} \sum_{k=0}^{2m} c_{jk} B_j^n(u) B_k^m(v), \tag{6}$$

where $c_{jk} \in \mathbb{R}^3$. The RKHS norm of $h$ in (6) is given by $||h||_{\mathbb{H}^{n,m}}^2 = \sum_{j=0}^{2n} \sum_{k=0}^{2m} \phi_{jk} ||c_{jk}||^2$.

*Proof of Theorem 7.* From Stepanets (1974) and observing that the basis functions $\{B_j^n, j = 0, \ldots, 2n\}$ span the vector space of trigonometric polynomials of degree at most $n$, it follows that given any $S_0^i \in C^{\alpha_i}(\mathbb{T}^2)$, there exists $h^i(u,v) = \sum_{j=0}^{2n} \sum_{k=0}^{2m} c_{jk}^i B_j^n(u) B_k^m(v)$, $h^i : \mathbb{T}^2 \to \mathbb{R}$ with $|c_{jk}^i| \leq M_i$, such that $||h^i - S_0^i||_\infty \leq K_i (n \wedge m)^{-\alpha_i} \log n \log m$ for some constants $M_i, K_i > 0, i = 1, 2, 3$. Setting $h(u,v) = \sum_{j=0}^{2n} \sum_{k=0}^{2m} (c_{jk}^1, c_{jk}^2, c_{jk}^3)^{\mathrm{T}} B_j^n(u) B_k^m(v)$, we have

$$||h - S_0||_\infty \leq M (n \wedge m)^{-\alpha_{(1)}} \log n \log m,$$

with $||h||_{\mathbb{H}}^2 \leq K \sum_{j=0}^{2n} \sum_{k=0}^{2m} \phi_{jk}$ where $M = M_{(3)}, K = K_{(3)}$.

*Proof of Theorem 9.* It is enough to verify the following along the lines of de Jonge and van Zanten (2010). We will show that if $S_0 \in \mathcal{S}_{\mathcal{C}}(\alpha_1, \alpha_2, \alpha_3)$ there exists for every constant $C > 1$ measurable subsets $B_N$ of $C(\mathbb{T}^2; \mathbb{R}^3)$ such that for $N$ large enough,

$$\log N(\bar{\epsilon}_N, B_N, ||\cdot||_\infty) \leq DN\bar{\epsilon}_N^2, \tag{7}$$

$$P(S \notin B_N) \leq e^{-CN\epsilon_N^2}, \tag{8}$$

$$P(\sup_{(u,v)\in\mathbb{T}^2} ||S(u,v) - S_0(u,v)|| \leq \epsilon_N) \geq e^{-N\epsilon_N^2}, \tag{9}$$

with $\epsilon_N = N^{-\alpha_{(1)}/(2\alpha_{(1)}+2)} \log^{t_1} N$ and $\bar{\epsilon}_N = N^{-\alpha_{(1)}/(2\alpha_{(1)}+2)} \log^{t_2} N$ for some global constants $t_1, t_2 > 0$. It is evident from de Jonge and van Zanten (2010) that the conditions (7) - (9) which are only related to the random object $S$ are alone sufficient to map to the general conditions on rates of contraction of posterior distributions used in Ghosal et al. (2000); Ghosal and van der Vaart (2007) assuming both $S_0$ and $\sigma_0$ to be unknown and $\sigma_0$ lying in some compact interval on which the prior for $\sigma$ is supported.

To find an upper bound to the metric entropy of the unit ball of $\mathbb{H}^{n,m}$, we embed it in an appropriate space of functions for which the upper bound is known. The function $h$ is in fact well defined on $\mathcal{A}(1) = \{z \in \mathbb{C}^2 : |Im(z_j)| \leq 1, j = 1, 2\}$, is analytic on this set and takes real values in $\mathbb{R}^2$. By the Cauchy-Schwartz inequality, it follows that with $\phi_{1,n,m} = \min\{\phi_{jk}, j = 0, \ldots, 2n, k = 0, \ldots, 2m\}$,

$$
\begin{aligned}
|h(z)|^2 &\leq \textstyle\sum_{j=0}^{2n} \sum_{k=0}^{2m} ||c_{jk}||^2 \phi_{jk} \sum_{j=0}^{2n} \sum_{k=0}^{2m} (1/\phi_{jk}) B_j^n(z_1)^2 B_k^m(z_2)^2, \\
&\leq ||h||^2_{\mathbb{H}^{n,m}} (1/\phi_{1,n,m}),
\end{aligned} \tag{10}
$$

for every $z \in \mathcal{A}(1)$. Let $\mathcal{S}(\phi, \psi)$ denote the set of all analytic functions on $\mathcal{A}(\psi)$, uniformly bounded by $\phi^{-0\cdot 5}$. (10) shows that $\mathbb{H}_1^{n,m} \subset \mathcal{S}(\phi_{1,n,m}, 1)$.

Next we characterize the metric entropy of $\mathcal{S}(\phi, \psi)$ for any $\phi > 0$ in Proposition 12.

**Proposition 12** *There exist $\epsilon_0, \phi_0 > 0$ such that*

$$
\log N(\epsilon, \mathcal{S}(\phi, \psi), || \cdot ||_\infty) \leq K_1 \frac{1}{\psi^2} \left( \log \frac{K_2}{\phi^{0\cdot 5} \epsilon} \right)^3
$$

*for $\phi \in (0, \phi_0)$ and $\epsilon \in (0, \epsilon_0)$.*

**Proof** The proof proceeds similarly to van der Vaart and van Zanten (2009). However, extra care is needed to identify the role of $\phi$ and $\psi$. Let $M = \phi^{-0\cdot 5}$. $h$ is an analytic function $h : \mathbb{C}^2 \to \mathbb{C}$, $|h(z)| \leq M$ for all $z \in \Omega = \{z \in \mathbb{C}^2 : |Re(z_1)| \leq \psi, |Re(z_2)| \leq \psi\}$ and hence admits a Taylor series expansion on $\Omega$.

Let $\{t_1, \ldots, t_m\}$ be an $\psi/2$-net of $\mathbb{T}^2$ for sup norm, let $\mathbb{T}^2 = \cup_{i=1}^m B_i$ be a partition of $\mathbb{T}^2$ into sets $B_1, \ldots, B_m$ obtained by assigning every $t \in \mathbb{T}^2$ to a closest $t_i \in \{t_1, \ldots, t_m\}$. Consider $P = \sum_{i=1}^m P_{i,a_i} I_{B_i}$ for $P_{i,a_i}(t) = \sum_{n. \leq k} a_{i,n}(t - t_i)^n$ where the sum ranges over $n = (n_1, n_2) \in (\mathbb{N} \cup \{0\})^2$ with $n. = n_1 + n_2 \leq k$ and $x^n$ is defined as $x_1^{n_1} x_2^{n_2}$. Obtain a finite set of functions by discretizing $a_{i,n}$ for each $i$ and $n$ over a mesh of $\epsilon/\psi^{n.}$-net of the interval $[-M/\psi^{n.}, M/\psi^{n.}]$. Then

$$
\log \left( \prod_i \prod_{n : n. \leq k} \# a_{i,n} \right) \leq \{3/(\psi/2)\}^2 k^2 \log \left( \frac{2M}{\epsilon} \right).
$$

By the Cauchy formula (2 applications of the formula in one dimension suffice), for $C_1, C_2$ circles of radius $\psi$ in the complex plane around the coordinates $t_{i1}, t_{i2}$ of $t_i$, and with $D^n$ the partial derivative of orders $n = (n_1, n_2)$ and $n! = n_1! n_2!$,

$$
\left| \frac{D^n h(t_i)}{n!} \right| = \left| \frac{1}{(2\pi i)^2} \oint_{C_1} \oint_{C_2} \frac{h(z)}{(z - t_i)^{n+1}} dz_1 dz_2 \right| \leq \frac{M}{\psi^{n.}}.
$$

Consequently for any $z \in B_i$, a universal constant $K$, an appropriately chosen $a_i$ and for $k > \log \frac{KM}{\epsilon}$,

$$
\left| \sum_{n. > k} \frac{D^n h(t_i)}{n!} (z - t_i)^n \right| \leq \sum_{n. > k} \frac{M}{\psi^{n.}} (\psi/2)^{n.} \leq M \sum_{l=k+1}^{\infty} \frac{l}{2^l} \leq KM \left( \frac{2}{3} \right)^k \leq \epsilon,
$$

$$
\left| \sum_{n. \leq k} \frac{D^n h(t_i)}{n!} (z - t_i)^n - P_{i,a_i}(z) \right| \leq \sum_{n. > k} \frac{\epsilon}{\psi^{n.}} (\psi/2)^{n.} \leq \epsilon \sum_{l=1}^{k} \frac{l}{2^l} \leq K\epsilon.
$$

Hence $\log N(\epsilon, \mathcal{S}(M,\psi), ||\cdot||_\infty) \leq K_1 \frac{1}{\psi^2}\big(\log \frac{K_2 M}{\epsilon}\big)^3$. ■

We return to verifying (7), (8) and (9). First we will verify (9). By Lemma 5.3 of van der Vaart and van Zanten (2008), we have for $S_0 \in \mathcal{S}_{\mathcal{C}}(\alpha_1, \alpha_2, \alpha_3)$, the inequality

$$-\log P(||S - S_0||_\infty < \epsilon) \leq \psi_{S_0}^{n,m}(\epsilon),$$

with $\psi_{S_0}^{n,m}$ denoting the *concentration function* defined as,

$$\psi_{S_0}^{n,m}(\epsilon) = \inf_{h \in \mathbb{H}^{n,m} : ||h - S_0||_\infty < \epsilon} ||h||^2_{\mathbb{H}^{n,m}} - \log P(||S^{n,m}|| < \epsilon).$$

We can provide a lower bound to $-\log P(||S^{n,m}|| < \epsilon)$ using Proposition 12. Observe that

$$P(||S - S_0|| \leq \epsilon_N) = \sum_{n,m=1}^{\infty} \Pi_{n,m} \int P(||S^{n,m} - S_0|| \leq \epsilon_N) \prod_{j,k=0}^{2n,2m} p(\phi_{jk}) d\phi_{jk}.$$

From Theorem 7 we obtain

$$P(||S - S_0|| \leq \epsilon_N) \geq \sum_{n,m \geq (1/\epsilon_N)^{1/\alpha_{(1)}}}^{\infty} \Pi_{n,m} \exp\bigg\{ - M(2n+1)(2m+1)\frac{\alpha_m \gamma_n}{\beta^2} + K_1 \bigg( \log \frac{K_3}{\epsilon_N}\bigg)^3 \bigg\}$$

for some constant $K_3 > 0$.

Next we will verify (8). Define $R_N$ to be the region $\{\phi_{jk} \geq t_N, j = 0, \ldots, n, k = 0, \ldots, m; n, m = 1, \ldots, r_N\}$, where $t_N$ and $r_N$ are to be determined. Let $\mathbb{B}_1$ denote the unit ball in the Banach space $C(\mathbb{T}^2; \mathbb{R}^3)$. Define

$$B_N = L_N \mathcal{S}(t_N, 1) + \epsilon_N \mathbb{B}_1.$$

Then by Borel's inequality (van der Vaart and van Zanten, 2008)

$$\begin{aligned}
P(S \notin B_N) &= \sum_{n=1}^{\infty}\sum_{m=1}^{\infty} \Pi_{n,m} \int P(S^{n,m} \notin B_N) \prod_{j,k=0}^{2n,2m} p(\phi_{jk}) d\phi_{jk} \\
&\leq \sum_{n=1}^{r_N}\sum_{m=1}^{r_N} \Pi_{n,m} \int P(S^{n,m} \notin L_N \mathbb{H}_1^{n,m} + \epsilon_N \mathbb{B}_1) \prod_{j,k=0}^{2n,2m} p(\phi_{jk}) d\phi_{jk} \\
&+ P(n > r_N, m > r_N) \\
&\leq \sum_{n=1}^{r_N}\sum_{m=1}^{r_N} \Pi_{n,m} \int_{R_N} P(S^{n,m} \notin L_N \mathbb{H}_1^{n,m} + \epsilon_N \mathbb{B}_1) \prod_{j,k=0}^{2n,2m} p(\phi_{jk}) d\phi_{jk} \\
&+ P(\phi_{1,r_N,r_N} \leq t_N) + P(n > r_N, m > r_N).
\end{aligned}$$

From van der Vaart and van Zanten (2009), the first term on the right hand side of the previous inequality is bounded as follows.

$$P(S^{n,m} \notin L_N \mathbb{H}_1^{n,m} + \epsilon_N \mathbb{B}_1) \leq 1 - \Phi[\Phi^{-1}\{P(||S^{n,m}||_\infty \leq \epsilon_N)\} + L_N].$$

For $\epsilon_N$ small enough and since $\Phi^{-1}(y) \geq -\{(5/2)\log(1/y)\}^{0\cdot5}$ for $y \in (0, 0\cdot5)$, it follows that

$$P(S^{n,m} \notin L_N \mathbb{H}_1^{n,m} + \epsilon_N \mathbb{B}_1) \leq 1 - \Phi\left[L_N - \left\{(5/2)K_1\left(\log \frac{K_2}{t_N^{0\cdot5}\epsilon_N}\right)^3\right\}^{0\cdot5}\right],$$

for $L_N \geq \left\{(5/2)K_1\left(\log \frac{K_2}{t_N^{0\cdot5}\epsilon_N}\right)^3\right\}^{0\cdot5}$ and for $\{\phi_{jk}, j = 0, \ldots, 2r_N, k = 0, \ldots, 2r_N\}$ in $R_N$.

Let $\tau_N = \min\{\tau_i, 0 \leq i \leq 2r_N\}, \tilde{\tau}_N \sim \mathrm{Ga}\{\alpha_{r_N}, (2r_N+1)\beta\}$ and $\kappa_N = \min\{\kappa_i, 0 \leq i \leq 2r_N\}, \tilde{\kappa}_N \sim \mathrm{Ga}\{\alpha_{r_N}, (2r_N+1)\beta\}$, $\tilde{\tau}_N$ and $\tilde{\kappa}_N$ are independent.

Observe that

$$\begin{aligned} P(\phi_{1,r_N,r_N} \leq t_N) &\leq P(\tau_N\kappa_N \leq t_N) \leq P(\tilde{\tau}_N\tilde{\kappa}_N \leq t_N) \\ &\leq \int_0^{e^{-1}} P(\tilde{\tau}_N \leq t_N/y) f_{\tilde{\kappa}_N}(y)dy + P(\tilde{\tau}_N \leq et_N). \end{aligned}$$

Now $P(\tilde{\tau}_N \leq et_N) \precsim \exp[\alpha_{r_N} + \alpha_{r_N}\log\{(2r_N+1)t_N\beta\} - \alpha_{r_N}\log\alpha_{r_N}]$ and $f_{\tilde{\kappa}_N}(y) \precsim \exp(-\alpha_{r_N})$ for $y \in (0, e^{-1})$. Thus

$$P(\phi_{1,r_N,r_N} \leq t_N) \precsim \exp[\alpha_{r_N} + \alpha_{r_N}\log\{(2r_N+1)t_N\beta\} - \alpha_{r_N}\log\alpha_{r_N}] + \exp(-\alpha_{r_N}).$$

Finally we will verify (7). For $\bar{\epsilon}_N \geq \epsilon_N$,

$$\begin{aligned} N(2\bar{\epsilon}_N, B_N, ||\cdot||_\infty) &\leq N(\bar{\epsilon}_N/L_N, \mathcal{S}(t_N, 1), ||\cdot||_\infty) \\ &\leq K_1\left(\log\frac{K_2}{t_N^{0\cdot5}\bar{\epsilon}_N/L_N}\right)^3. \end{aligned}$$

Letting $\gamma_N = O(\log N)^3, r_N = O\left\{\exp\left(N^{\frac{2}{3(2\alpha_{(1)}+2)}}\right)\right\}, t_N = O\left\{\exp\left(-N^{\frac{2}{3(2\alpha_{(1)}+2)}}\right)\right\}$ such that $(2r_N+1)t_N\beta$ is a global constant, $L_N^2 = N^{2/(2\alpha_{(1)}+2)}$, we can verify that (7), (8) and (9) are satisfied with $\epsilon_N = N^{-\alpha_{(1)}/(2\alpha_{(1)}+2)}\log^{t_1} N$ and $\bar{\epsilon}_N = N^{-\alpha_{(1)}/(2\alpha_{(1)}+2)}\log^{t_2} N$ for some global constants $t_1, t_2 > 0$. $P(n > r_N, m > r_N)$ is guaranteed to be $O\left[\exp\left\{-N^{\frac{2}{2\alpha_{(1)}+2}}\right\}\right]$ from the tail condition in the assumption.

## References


N. Amenta, M. Bern, and M. Kamvysselis. A new voronoi-based surface reconstruction algorithm. In *Proceedings of the 25th annual conference on Computer graphics and interactive techniques*, pages 415–421. ACM, 1998.

N.M. Aziz, R. Bata, and S. Bhat. Bezier surface/surface intersection. *Computer Graphics and Applications, IEEE*, 10(1):50–58, 2002.

RE Barnhill. Surfaces in computer aided geometric design: A survey with new results. *Computer Aided Geometric Design*, 2(1-3):1–17, 1985.

J.D. Boissonnat and S. Oudot. Provably good sampling and meshing of surfaces. *Graphical Models*, 67(5):405–451, 2005.

C. Brechbühler, G. Gerig, and O. Kübler. Parametrization of closed surfaces for 3-D shape description. *Computer vision and image understanding*, 61(2):154–170, 1995.

M.S. Casale. Free-form solid modeling with trimmed surface patches. *Computer Graphics and Applications, IEEE*, 7(1):33–43, 1987.

M.K. Chung, K.M. Dalton, and R.J. Davidson. Tensor-based cortical surface morphometry via weighted spherical harmonic representation. *IEEE Transactions on Medical Imaging*, 27(8):1143–1151, 2008.

P. Cinquin, B. Chalmond, D. Berard, L. Dusserre, P. Trouilloud, P. Grammont, D. Binnert, JP Mabille, and C. Carasso. Hip prosthesis design. *Lecture Notes in Medical Informatics*, 16:195–200, 1982.

G.S. Cunningham, A. Lehovich, and K.M. Hanson. Bayesian estimation of regularization parameters for deformable surface models. In *Proc. SPIE*, volume 3661, pages 562–573. Citeseer, 1999.

R. de Jonge and JH van Zanten. Adaptive nonparametric Bayesian inference using location-scale mixture priors. *The Annals of Statistics*, 38(6):3300–3320, 2010.

DGT Denison, BK Mallick, and AFM Smith. Bayesian MARS. *Statistics and Computing*, 8(4):337–346, 1998.

Gerald Farin. *Curves and surfaces for CAGD: a practical guide*. Morgan Kaufmann Publishers Inc., San Francisco, CA, USA, 5th edition, 2002. ISBN 1-55860-737-4.

B. Fowler. Geometric manipulation of tensor product surfaces. In *Proceedings of the 1992 symposium on Interactive 3D graphics*, pages 101–108. ACM, 1992.

S. Ghosal and A. van der Vaart. Convergence rates of posterior distributions for noniid observations. *The Annals of Statistics*, 35(1):192–223, 2007.

S. Ghosal, J.K. Ghosh, and A.W. van der Vaart. Convergence rates of posterior distributions. *Annals of Statistics*, 28(2):500–531, 2000.

S.J. Godsill. On the relationship between Markov chain Monte Carlo methods for model uncertainty. *Journal of Computational and Graphical Statistics*, 10(2):230–248, 2001.

W.J. Gordon and R.F. Riesenfeld. Bernstein-Bézier methods for the computer-aided design of free-form curves and surfaces. *Journal of the ACM (JACM)*, 21(2):293–310, 1974.

A. Goshtasby. Surface reconstruction from scattered measurements. In *Proc. SPIE*, volume 1830, pages 247–256. Citeseer, 1992.

H. Hagen and P. Santarelli. Variational design of smooth B-spline surfaces. In *Topics in surface modeling*, pages 85–92. Society for Industrial and Applied Mathematics, 1992. ISBN 0898712823.

H. Hoppe, T. DeRose, T. Duchamp, J. McDonald, and W. Stuetzle. Surface reconstruction from unorganized points. *Computer Graphics*, 26:71–71, 1992.

J.K. Johnstone and K.R. Sloan. Tensor product surfaces guided by minimal surface area triangulations. In *Visualization*, page 254. Published by the IEEE Computer Society, 1995.

M. Kazhdan, M. Bolitho, and H. Hoppe. Poisson surface reconstruction. In *Proceedings of the fourth Eurographics symposium on Geometry processing*, pages 61–70. Eurographics Association, 2006.

J. Lang and O. Röschel. Developable (1, n)-Bézier surfaces. *Computer Aided Geometric Design*, 9(4):291–298, 1992.

J.X. Li. Visualization of high-dimensional data with relational perspective map. *Information Visualization*, 3(1):49–59, 2004.

R. Li, G. Li, and Y. Wang. Closed surface modeling with helical line measurement data. *Frontiers of Mechanical Engineering in China*, 2(1):72–76, 2007.

W.E. Lorensen and H.E. Cline. Marching cubes: A high resolution 3D surface construction algorithm. In *Proceedings of the 14th annual conference on Computer graphics and interactive techniques*, pages 163–169. ACM, 1987. ISBN 0897912276.

S. Mann and T. DeRose. Computing values and derivatives of Bézier and B-spline tensor products. *Computer Aided Geometric Design*, 12(1):107–110, 1995.

H. Muller. Surface reconstruction-an introduction. In *Scientific Visualization Conference, 1997*, page 239. IEEE, 2005. ISBN 0769505031.

L. Piegl. The sphere as a rational Bezier surface. *Computer Aided Geometric Design*, 3(1): 45–52, 1986.

L. Rineau and M. Yvinec. A generic software design for Delaunay refinement meshing. *Computational Geometry*, 38(1-2):100–110, 2007.

D. Rossi and A. Willsky. Reconstruction from projections based on detection and estimation of objects–Parts I and II: Performance analysis and robustness analysis. *Acoustics, Speech and Signal Processing, IEEE Transactions on*, 32(4):886–906, 2003.

Á. Róth and I. Juhász. Control point based exact description of a class of closed curves and surfaces. *Computer Aided Geometric Design*, 27(2):179–201, 2010.

Á. Róth, I. Juhász, J. Schicho, and M. Hoffmann. A cyclic basis for closed curve and surface modeling. *Computer Aided Geometric Design*, 26(5):528–546, 2009.

T.W. Sederberg. Implicit and parametric curves and surfaces for computer aided geometric design. *ETD Collection for Purdue University*, 1983.

L. Shen and F. Makedon. Spherical mapping for processing of 3D closed surfaces. *Image and vision computing*, 24(7):743–761, 2006.

M. Smith and R. Kohn. A Bayesian approach to nonparametric bivariate regression. *Journal of the American Statistical Association*, 92(440):1522–1535, 1997.

C. Soussen and A. Mohammad-Djafari. Closed surface reconstruction in X-ray tomography. In *Image Processing, 2001. Proceedings. 2001 International Conference on*, volume 1, pages 718–721. IEEE, 2002. ISBN 0780367251.

AI Stepanets. The approximation of certain classes of differentiable periodic functions of two variables by fourier sums. *Ukrainian Mathematical Journal*, 25(5):498–506, 1974.

B. Su and D. Liu. *Computational geometry: curve and surface modeling.* Academic Press Professional, Inc. San Diego, CA, USA, 1989. ISBN 0126756104.

R. Szeliski and D. Tonnesen. Surface modeling with oriented particle systems. *ACM SIGGRAPH Computer Graphics*, 26(2):185–194, 1992.

AW van der Vaart and JH van Zanten. Reproducing kernel Hilbert spaces of Gaussian priors. *IMS Collections*, 3:200–222, 2008.

A.W. van der Vaart and J.H. van Zanten. Adaptive Bayesian estimation using a Gaussian random field with inverse Gamma bandwidth. *The Annals of Statistics*, 37(5B):2655–2675, 2009.

K.Y. Whang, J.W. Song, J.W. Chang, J.Y. Kim, W.S. Cho, C.M. Park, and I.Y. Song. Octree-R: An adaptive octree for efficient ray tracing. *Visualization and Computer Graphics, IEEE Transactions on*, 1(4):343–349, 2002.

M. Yang and E. Lee. Segmentation of measured point data using a parametric quadric surface approximation. *Computer Aided Design*, 31(7):449–457, 1999.